

## **Chapter VI**

### ***Laplace Analysis of Periodic Heat and Mass Transport on a Parabolic Started Surface immersed in Darcian Porous Regime***

**Some part of this chapter has been published in the UGC approved journal entitled- International Journal of Engineering Research and Application, Volume 7- Issue 4 (Part-IV), April 2017, PP 85-89**

## 6.1 Introduction:

Transport processes in porous media can involve fluid, heat and mass transfer in single or multi-phase scenarios. Such flows with and without buoyancy effects arise frequently in many branches of chemical engineering and owing to their viscous-dominated nature are generally simulated using the Darcy model. Applications of such flows include chip-based micro fluidic chromatographic separation devices (2002), dissolution of masses buried in a packed bed (2007), heat transfer in radon saturating permeable regimes (2003), flows in ceramic filter components of integrated gasification combined cycles (IGCC) (1998), separation of carbon dioxide from the gas phase with aqueous adsorbents (water and diethanolamine solution) in micro porous hollow fibre membrane modules (1997), food processing and polymer production. Keeping in view these applications Chamkha *et al.* (2000) studied the effects of Hydro magnetic combined heat and mass transfer by natural convection from a permeable surface embedded in a fluid saturated porous medium. Mukherjee *et al.* (2014) studied the momentum and the heat transfer characteristics in incompressible electrically conducting boundary layer flow over an exponentially stretching sheet under the effect of magnetic field with thermal radiation through porous medium. Ahmed (2010) investigated the effect of periodic heat transfer on unsteady MHD mixed convection flow past a vertical porous flat plate with constant suction and heat sink when the free stream velocity oscillates in about a non-zero constant mean.

There are many applications for the parabolic motion such as solar cookers, solar concentrators and parabolic trough solar collector. A parabolic concentrator type solar cooker has a wide range of applications like baking, roasting and distillation due to its unique property of producing a practically higher temperature of nearly  $250^{\circ}\text{C}$  and hence it provides inconvenience to the user due to high amount of glare. Solar concentrators have their applications in increasing the rate of evaporation of waste water, in food processing, for making drinking water from brackish and sea water. Many researchers have been attracted due to these important applications namely Kumar *et al.* (2015) investigated about the viscous dissipation effects on the unsteady magnetohydrodynamic free convective flow past a parabolic starting motion of the infinite vertical plate with

variable temperature and variable mass diffusion. Muthucumaraswamy *et al.* (2014a) presented an exact solution of unsteady flow past a parabolic starting motion of an infinite vertical plate with variable temperature and mass diffusion, in the presence of a homogeneous chemical reaction of first order. Muralidharan *et al.* (2014) presented a closed form solution of flow past a parabolic starting motion of the infinite vertical plate with uniform heat flux and variable mass diffusion. Muthucumaraswamy *et al.* (2014) investigated the hypothetical solution of flow past a parabolic starting motion of the infinite vertical plate with variable temperature and variable mass diffusion. Muthucumaraswamy *et al.* (2013) studied an exact solution of unsteady flow past a parabolic started infinite isothermal vertical plate with uniform mass flux, in the presence of thermal radiation.

Magnetohydrodynamic flows in porous media have stimulated considerable attention owing to the importance of such flows in magnetic materials processing (1977), chemical engineering (1989) and geophysical energy systems (1994). In view of these applications of the flow through porous medium, a series of investigation has been made by Raptis *et al.* (1981, 1982, 1989), where the porous medium is either bounded by horizontal, vertical surfaces or parallel porous plates. Ahmed (2013) investigated the unsteady hydromagnetic flow of an electrically conducting fluid through a *Darcian* porous medium adjacent to a uniformly accelerated vertical plate in a rotating system using boundary layer approximation. Chaudhary and Jain (2008) studied the influence of oscillating temperature on magnetohydrodynamic convection heat transfer past a vertical plane in a *Darcian* porous medium. An investigation was performed for unsteady Magnetohydrodynamic boundary layer flow and heat transfer through a *Darcian* porous medium bounded by a uniformly moving semi-infinite isothermal vertical plate in presence of thermal radiation by Khatun and Ahmed (2015).

Mass diffusion rates can be changed tremendously with chemical reactions. The chemical reaction effects depend whether the reaction is homogeneous or heterogeneous. This depends on whether they occur at an interface or as a single phase volume reaction. In well mixed systems, the reaction is heterogeneous, if it takes place at an interface and homogeneous, if it takes place in solution. In majority cases, a chemical reaction depends

on the concentration of the species itself. A reaction is said to be of first order, if the rate of reaction is directly proportional to the concentration of only one reactant and is independent of others. Decomposition of nitrogen pent oxide in the gas phase as well in an organic solvent like  $\text{CCl}_4$ , conversion of N-chloroacetanilide into p-chloroacetanilide, hydrolysis of methyl acetate and inversion of cane sugar. The radioactive disintegration of unstable nuclei are the best examples of first order reactions. The related literatures are Agrawal *et al.* (1998) studied free convection due to thermal and mass diffusion in laminar flow of an accelerated infinite vertical plate in the presence of magnetic field. Agrawal *et al.* (1999) further extended the problem of unsteady free convective flow and mass diffusion of an electrically conducting elasto-viscous fluid past a parabolic starting motion of the infinite vertical plate with transverse magnetic field. The governing equations are tackled using Laplace transform technique. Muthucumaraswamy *et al.* (2015) studied on the unsteady hydromagnetic flow past a parabolic starting motion of the infinite vertical plate with variable temperature and mass diffusion, in the presence of homogeneous chemical reaction of first order.

The aim of the present problem is to investigate the effects of porosity of the medium and chemical reaction on the flow past an infinite vertical plate subjected to parabolic motion with variable temperature, in the presence of applied transverse magnetic field. The dimensionless governing equations are solved using the Laplace-transform technique. The solutions are derived in terms of exponential and complementary error functions. The validity of the present flow model has been established through the results compared with the results of the previous work done by Muthucumaraswamy and Velmurugan (2015) and the results are in good agreement.

## 6.2 Mathematical Analysis:

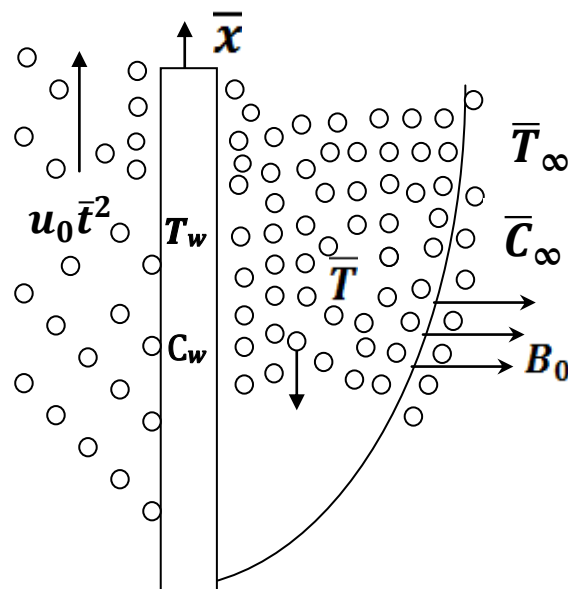
In this problem, we consider the unsteady hydromagnetic flow of a viscous incompressible fluid past an infinite vertical plate with variable temperature and mass diffusion, in the presence of chemical reaction of first order and applied transverse magnetic field. The  $\bar{x}$  -axis is taken along the plate in the vertically upward direction and the  $\bar{y}$  -axis is taken normal to the plate. At time  $\bar{t} \leq 0$ , the plate and fluid are at the same temperature  $T_\infty$  and concentration  $\bar{C}_\infty$ . At time  $\bar{t} > 0$ , the plate is started with a velocity  $\bar{u} = u_0 \bar{t}^2$  in its own plane against gravitational field. The plate temperature as well as concentration near the plate is raised linearly with time. A chemically reactive species which transforms according to a simple reaction involving the concentration is emitted from the plate and diffuses into the fluid. The plate is also subjected to a uniform magnetic field of strength  $B_0$  is assumed to be applied normal to the plate. The reaction is assumed to take place entirely in the stream. Then under usual Boussinesq's approximation for unsteady parabolic starting motion is governed by the following equations (Muthucumaraswamy and Velmurugan (2015)):

$$\frac{\partial \bar{u}}{\partial \bar{y}} = 0 \quad (6.2.1)$$

$$\frac{\partial \bar{u}}{\partial \bar{t}} = g\beta(\bar{T} - \bar{T}_\infty) + g\beta(\bar{C} - \bar{C}_\infty) + \nu \frac{\partial^2 \bar{u}}{\partial \bar{y}^2} - \frac{\sigma B_0^2}{\rho} \bar{u} - \frac{\nu}{K} \bar{u} , \quad (6.2.2)$$

$$\rho C_p \frac{\partial \bar{T}}{\partial \bar{t}} = \kappa \frac{\partial^2 \bar{T}}{\partial \bar{y}^2} , \quad (6.2.3)$$

$$\frac{\partial \bar{C}}{\partial \bar{t}} = D \frac{\partial^2 \bar{C}}{\partial \bar{y}^2} - \bar{C}_r(\bar{C} - \bar{C}_\infty) . \quad (6.2.4)$$



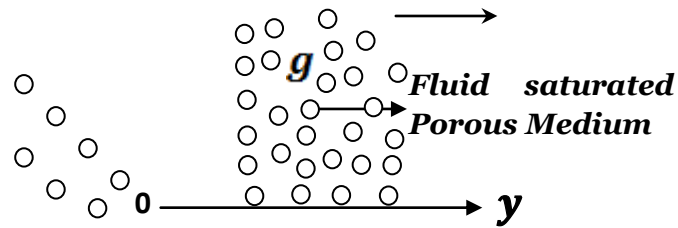


**Fig. 6.2 (i): Physical model and coordinate system**

The magnetic and viscous dissipations are neglected in this study. The first and second terms on the RHS of the momentum equation (6.2.1) denote the thermal and concentration buoyancy effects, respectively. It is assumed that the permeable plate moves with a variable velocity in the direction of fluid flow. In addition, it is assumed that the temperature and the concentration at the wall are varying with time.

The initial and boundary conditions are:

$$\left\{ \begin{array}{l} (\bar{u} = 0, \bar{T} = \bar{T}_\infty, \bar{C} = \bar{C}_\infty) \text{ for all } \bar{y}, \bar{t} \leq 0 \\ \bar{t} > 0 : \left( \begin{array}{l} \bar{u} = u_0 \bar{t}^2, \bar{T} = \bar{T}_\infty + (\bar{T}_w - \bar{T}_\infty) A \bar{t}, \\ \bar{C} = \bar{C}_\infty + (\bar{C}_w - \bar{C}_\infty) A \bar{t} \end{array} \right) \text{ at } \bar{y} = 0 \\ \bar{t} > 0 : (\bar{u} \rightarrow 0, \bar{T} \rightarrow \bar{T}_\infty, \bar{C} \rightarrow \bar{C}_\infty) \text{ as } \bar{y} \rightarrow \infty \end{array} \right\}, \quad (6.2.5)$$

where  $A = \left( \frac{u_0^2}{\nu} \right)^{1/3}$  Muthucumaraswamy and Velmurugan (2015).

On introducing the following non-dimensional quantities

$$\left\{ \begin{array}{l} u = \bar{u} \left( \frac{u_0}{v^2} \right)^{\frac{1}{3}}, \quad t = \bar{t} \left( \frac{u_0^2}{v} \right)^{\frac{1}{3}}, \quad y = \bar{y} \left( \frac{u_0}{v^2} \right)^{\frac{1}{3}}, \quad \theta = \frac{T - T_\infty}{T_w - T_\infty}, \\ C = \frac{\bar{C} - \bar{C}_\infty}{\bar{C}_w - \bar{C}_\infty}, \quad Gr = \frac{g\beta(T_w - T_\infty)}{(vu_0)^{\frac{1}{3}}}, \quad Gm = \frac{g\beta(\bar{C}_w - \bar{C}_\infty)}{(vu_0)^{\frac{1}{3}}}, \\ K = \bar{K} \left( \frac{u_0}{v^2} \right)^{\frac{2}{3}}, \quad M = \frac{\sigma B_0^2}{\rho} \left( \frac{v}{u_0^2} \right)^{\frac{1}{3}}, \quad C_r = \bar{C}_r \left( \frac{v}{u_0^2} \right)^{\frac{1}{3}}, \\ Pr = \frac{\mu C_p}{\kappa}, \quad Sc = \frac{v}{D}, \end{array} \right. \quad (6.2.6)$$

The dimensional equations (6.2.2) - (6.2.3) reduces to the following non-dimensional form

$$\frac{\partial u}{\partial t} = Gr\theta + GmC + \frac{\partial^2 u}{\partial y^2} - (M + K^{-1})u \quad (6.2.7)$$

$$\frac{\partial \theta}{\partial t} = \frac{1}{Pr} \frac{\partial^2 \theta}{\partial y^2} \quad (6.2.8)$$

$$\frac{\partial C}{\partial t} = \frac{1}{Sc} \frac{\partial^2 C}{\partial y^2} - C_r C \quad (6.2.9)$$

The corresponding initial and boundary conditions in non-dimensional form are as follows

$$\left\{ \begin{array}{l} (u = 0, \theta = 0, C = 0) \text{ for all } y, t \leq 0 \\ t > 0 : (u = t^2, \theta = t, C = t) \text{ at } y = 0 \\ t > 0 : (u \rightarrow 0, \theta \rightarrow 0, C \rightarrow 0) \text{ as } y \rightarrow \infty \end{array} \right. \quad (6.2.10)$$

### 6.3 Methodology:

The equations (6.2.7) - (6.2.9) and the corresponding initial and boundary conditions (6.2.10) are solved by the Laplace-transform technique and consequently the solutions obtained as follows:

$$\theta = t \left[ (1 + 2\eta^2 Pr) \operatorname{erfc}(\eta\sqrt{Pr}) - \frac{2\eta\sqrt{Pr}}{\sqrt{\pi}} \exp(-\eta^2 Pr) \right] \quad (6.3.1)$$

$$C = \left\{ \begin{array}{l} \frac{t}{2} \exp(2\eta\sqrt{ScC_r t}) \operatorname{erfc}(\eta\sqrt{Sc} + \sqrt{C_r t}) \\ \frac{t}{2} \exp(-2\eta\sqrt{ScC_r t}) \operatorname{erfc}(\eta\sqrt{Sc} - \sqrt{C_r t}) \\ - \frac{\eta\sqrt{Sc}\sqrt{t}}{2\sqrt{C_r}} \exp(-2\eta\sqrt{ScC_r t}) \operatorname{erfc}(\eta\sqrt{Sc} - \sqrt{C_r t}) \\ + \frac{\eta\sqrt{Sc}\sqrt{t}}{2\sqrt{C_r}} \exp(-2\eta\sqrt{ScC_r t}) \operatorname{erfc}(\eta\sqrt{Sc} + \sqrt{C_r t}) \end{array} \right\}, \quad (6.3.2)$$

$$u = \left\{ \begin{aligned} & \left[ \frac{\eta^2 + Nt(1 + 2ac + 2bd) + 2N(c + d)}{2N} \right] \\ & \left[ \begin{aligned} & \exp\{2\eta\sqrt{Nt}\} \operatorname{erfc}\{\eta + \sqrt{Nt}\} \\ & + \exp\{-2\eta\sqrt{Nt}\} \operatorname{erfc}\{\eta - \sqrt{Nt}\} \end{aligned} \right] \\ & + \left[ \frac{\eta\sqrt{t}\{1 - 4N(t + ac + bd)\}}{4N^{\frac{3}{2}}} \right] \\ & \left[ \begin{aligned} & \exp\{-2\eta\sqrt{Nt}\} \operatorname{erfc}\{\eta - \sqrt{Nt}\} \\ & - \exp\{2\eta\sqrt{Nt}\} \operatorname{erfc}\{\eta + \sqrt{Nt}\} \end{aligned} \right] \\ & - \frac{\eta t}{N\sqrt{\pi}} \exp\{-\eta^2 + Nt\} - 2c \operatorname{erfc}(\eta\sqrt{Pr}) \\ & - 2act \left[ (1 + 2\eta^2 Pr) \operatorname{erfc}(\eta\sqrt{Pr}) - \frac{2(\eta\sqrt{Pr})}{\sqrt{\pi}} \exp(-\eta^2 Pr) \right] \\ & + c \exp(at) \left[ \begin{aligned} & \exp\{2\eta\sqrt{\{N+a\}t}\} \operatorname{erfc}\{\eta + \sqrt{\{N+a\}t}\} \\ & + \exp\{-2\eta\sqrt{\{N+a\}t}\} \operatorname{erfc}\{\eta - \sqrt{\{N+a\}t}\} \end{aligned} \right] \\ & - d \exp(bt) \left[ \begin{aligned} & \exp\{2\eta\sqrt{\{N+b\}t}\} \operatorname{erfc}\{\eta + \sqrt{\{N+b\}t}\} \\ & + \exp\{-2\eta\sqrt{\{N+b\}t}\} \operatorname{erfc}\{\eta - \sqrt{\{N+b\}t}\} \end{aligned} \right] \\ & + c \exp(at) \left[ \begin{aligned} & \exp(2\eta\sqrt{Prat}) \operatorname{erfc}(\eta\sqrt{Pr} + \sqrt{at}) \\ & + \exp(-2\eta\sqrt{Prat}) \operatorname{erfc}(\eta\sqrt{Pr} - \sqrt{at}) \end{aligned} \right] \\ & + d \exp(bt) \\ & \left[ \begin{aligned} & \exp(2\eta\sqrt{Sc(C_r + b)t}) \operatorname{erfc}(\eta\sqrt{Sc} + \sqrt{(C_r + b)t}) \\ & + \exp(-2\eta\sqrt{Sc(C_r + b)t}) \operatorname{erfc}(\eta\sqrt{Sc} - \sqrt{(C_r + b)t}) \end{aligned} \right] \\ & - (1 + bt)d \left[ \begin{aligned} & \exp(2\eta\sqrt{ScC_r t}) \operatorname{erfc}(\eta\sqrt{Sc} + \sqrt{C_r t}) \\ & + \exp(-2\eta\sqrt{ScC_r t}) \operatorname{erfc}(\eta\sqrt{Sc} - \sqrt{C_r t}) \end{aligned} \right] \\ & + \frac{bd\eta\sqrt{Sc}\sqrt{t}}{\sqrt{K}} \left[ \begin{aligned} & \exp(-2\eta\sqrt{ScC_r t}) \operatorname{erfc}(\eta\sqrt{Sc} - \sqrt{C_r t}) \\ & - \exp(2\eta\sqrt{ScC_r t}) \operatorname{erfc}(\eta\sqrt{Sc} + \sqrt{C_r t}) \end{aligned} \right] \end{aligned} \right\} \quad (6.3.3)$$

Where

$$N = M + K^{-1}, \quad a = \frac{N}{Pr - 1}, \quad b = \frac{(M + K^{-1}) - C_r Sc}{Sc - 1},$$

$$sc = \frac{Gr}{2a^2(1 - Pr)}, \quad d = \frac{Gm}{2b^2(1 - Sc)}, \quad \eta = \frac{y}{2\sqrt{t}}$$

## 6.4 Validity:

The comparison of the present work with the previous work done by Muthucumaraswamy and Velmurugan (2015) is presented in Table-6.4(a) without *porosity* of the medium when  $Gr = Gm = 5$ ,  $M = 5$ ,  $t = 0.2$ ,  $C_r = 0.1$ :

y	Present work			Muthucumaraswamy and Velmurugan (2015)		
	$Pr = 0.2$	$Pr = 0.4$	$Pr = 0.6$	$Pr = 0.2$	$Pr = 0.4$	$Pr = 0.6$
0	0.285895	0.239544	0.207347	0.285885	0.239538	0.207319
0.2	0.225094	0.188194	0.160509	0.225061	0.188159	0.160511
0.4	0.163767	0.135083	0.113088	0.163753	0.135090	0.113072
0.6	0.110581	0.0888176	0.072593	0.110577	0.088828	0.072574
0.8	0.069761	0.053565	0.042375	0.069777	0.053565	0.042375
1	0.04162	0.0297211	0.022444	0.04154	0.029735	0.022451

The comparison of the present results with previously published work has established the good agreement and it has been observed that the absolute difference between these comparisons for the flow velocity is less than  $10^{-5}$ . It is seen from the Table-6.4(a) that the flow velocity are decreased with the increasing values of Prandtl number ( $Pr$ ).

## 6.5 Results and Discussion:

In order to get a clear insight of the physical problem, numerical results are displayed with the help of graphs in details. This enables us to carry out the numerical calculations for the distribution of the velocity, temperature and concentration across the boundary layer for various values of the parameters. In the present study we have chosen  $M = 5$ ,  $Gr = Gm = 5$ ,  $t = 0.1$ ,  $K = 0.1$ ,  $Sc = 0.6$ ,  $Pr = 0.71$  and  $C_r = 0.1$ .

The effect of the Hartmann number  $M$  on the dimensionless velocity profile  $u$  has been presented in Fig. 6.5 (i). It is observed in this Figure that the velocity is decreased with the increase of the magnetic parameter. The effects of a transverse magnetic field give rise to a resistive-type force called the Lorentz force. This force has the tendency to slow down the motion of the fluid flow.

Figure 6.5 (ii) shows the velocity profiles for different values of the permeability ( $K$ ). Clearly the increasing  $K$  gets the peak value of velocity. These results could be very useful in deciding the applicability of enhanced oil recovery in reservoir engineering.

Figure 6.5 (iii) depicts the effects of the local thermal free convection ( $Gr$ ) with increasing  $y$  on the dimensionless velocity. It is observed that the increase of the Grashoff number leads to the increase of the velocity of the fluid. This is because the increase of  $Gr$  results in the increase of temperature gradients ( $T_w - T_\infty$ ), leads to the enhancement of the velocity due to the enhanced convection.

A typical variation of the temperature profile along the span wise coordinate  $y$  is shown in Fig. 6.5 (iv) for different values of Prandtl number ( $Pr$ ). The results show that an increase of Prandtl number decreases the temperature profiles of thermal boundary layer thickness and more uniform temperature distribution across the boundary layer. Moreover, the velocity becomes linear due to the metallic liquid ( $Pr = 0.25$ ).

The effects of the generative chemical reaction parameter  $C_r$  on the dimensionless velocity  $u$  and concentration  $\phi$  profiles are respectively presented in Figs 6.5 (v) and 6.5 (vi). It is observed in these Figures that the velocities as well as concentration are decreased with the increase of the generative chemical reaction. The effect of chemical

reaction parameter is very important in the concentration field. Chemical reaction increases the rate of interfacial mass transfer. Reaction reduces the local concentration, thus increases its concentration gradient and its flux.

Figure 6.5 (vii) illustrates the concentration profiles across the boundary layer for various values of Schmidt number  $Sc$ . The figure shows that increasing  $Sc$  results decreases the concentration distribution, because the smaller values of  $Sc$  are equivalent to increasing the chemical molecular diffusivity.

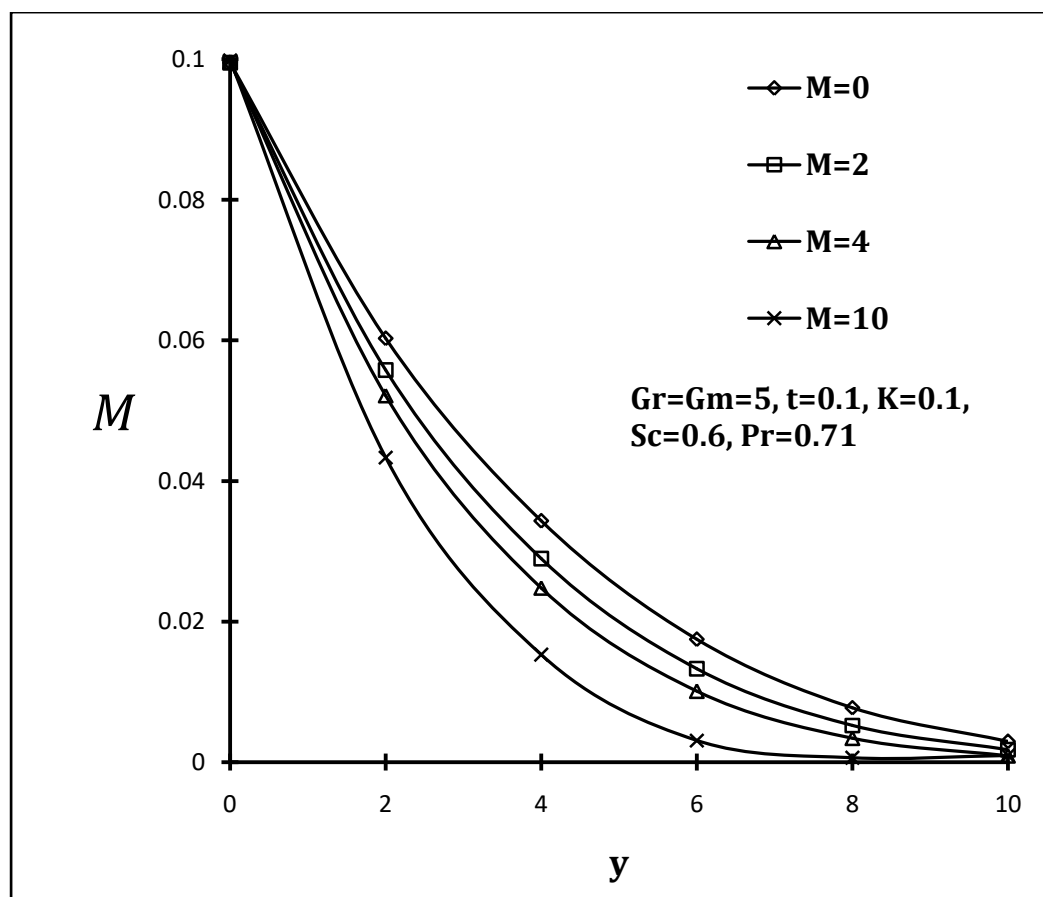


**Fig. 6.5(i): Velocity profile for magnetic field,  $M$**

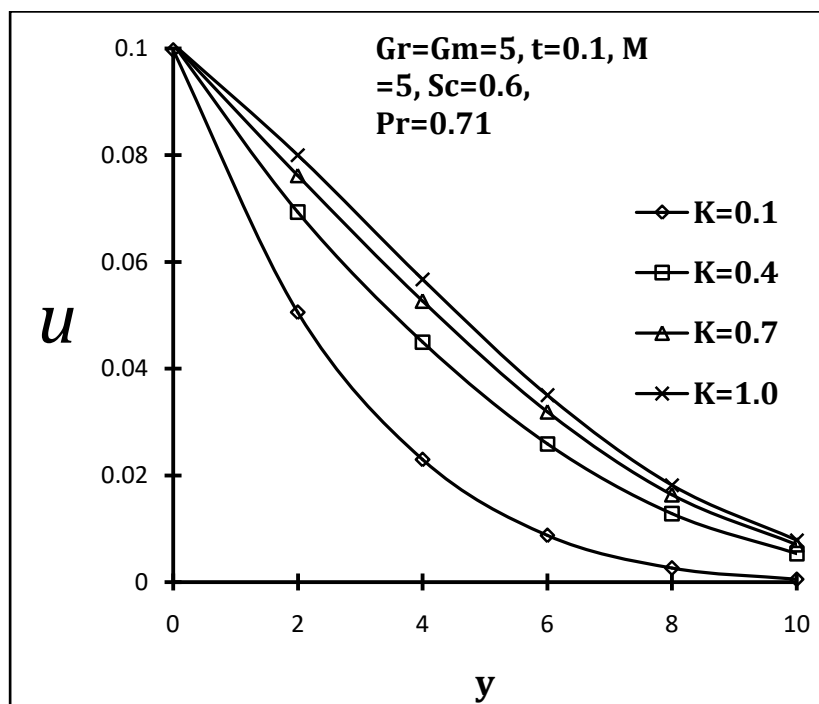


Fig. 6.5 (ii): Velocity profile for porosity,  $K$

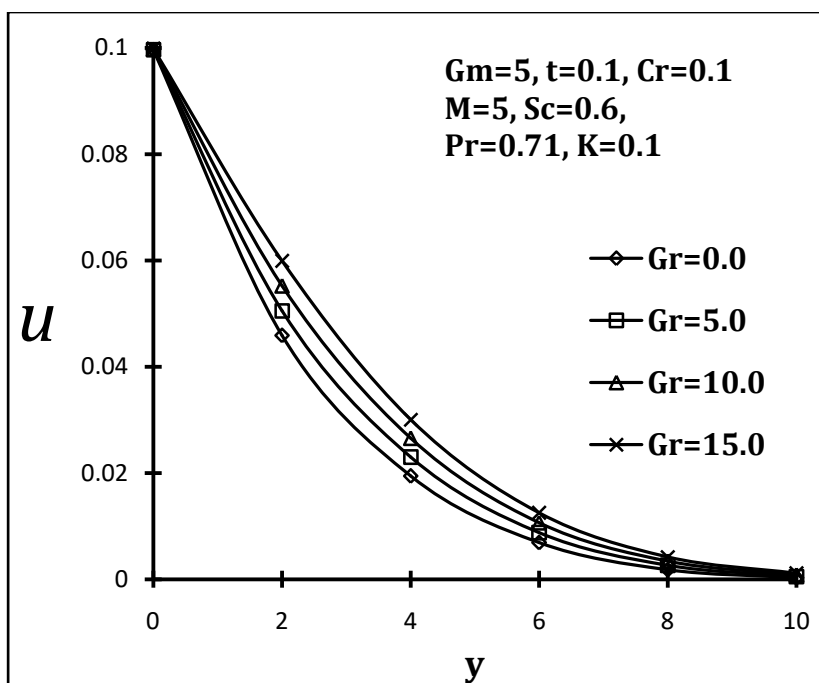
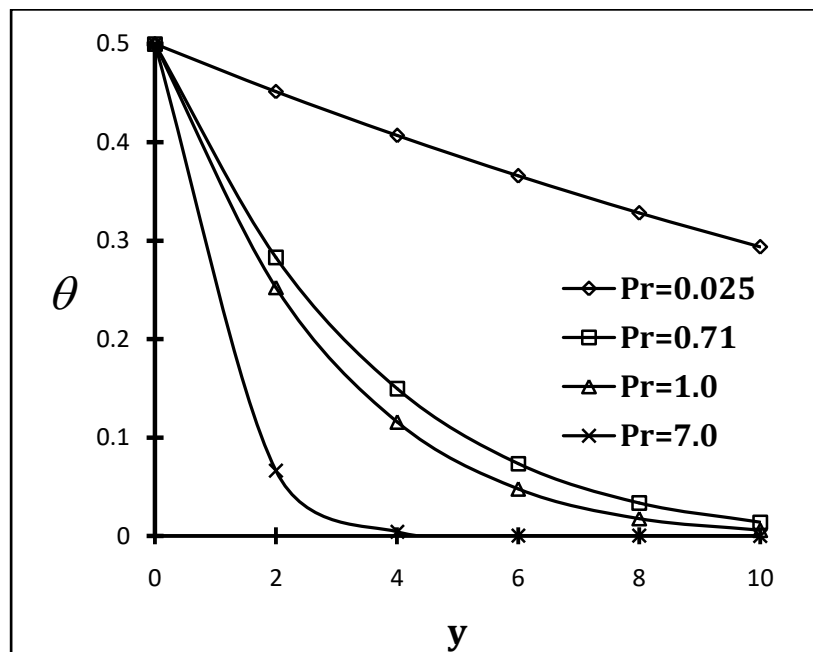
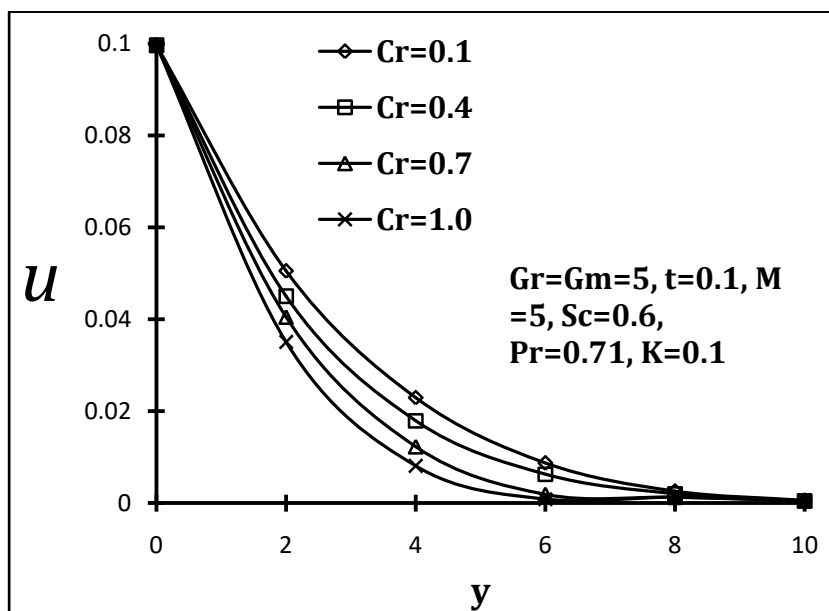


Fig. 6.5 (iii): Velocity profile for free convection parameter,  $Gr$



**Fig. 6.5 (iv):** Temperature profile for Prandtl parameter,  $Pr$



**Fig. 6.5 (v):** Velocity profile for chemical reaction,  $Cr$

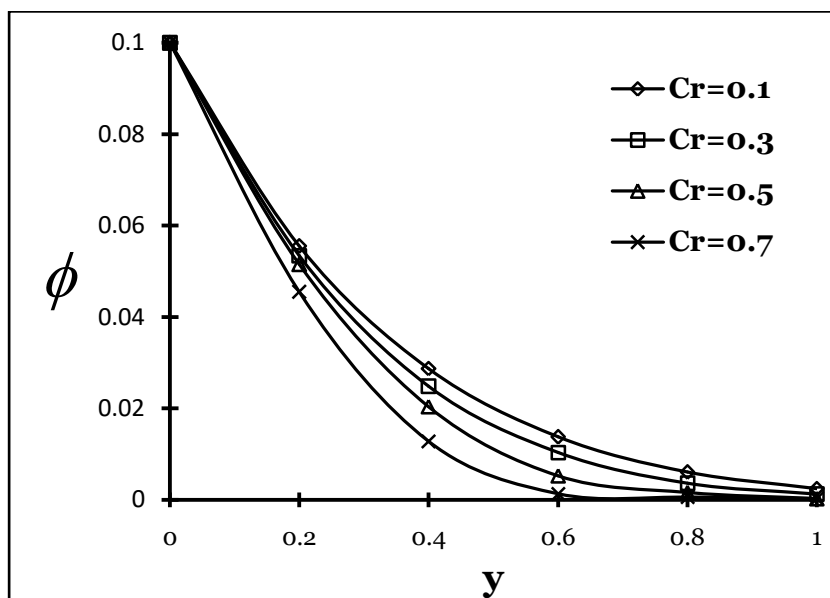


**Fig. 6.5 (vi):** Concentration profile for chemical reaction,  $C_r$

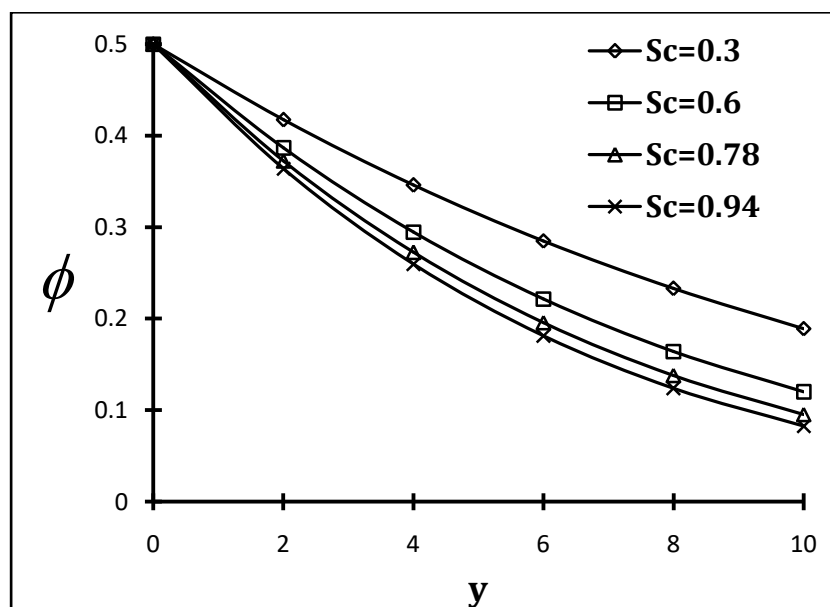


**Fig. 6.5 (vii):** Concentration profile for Schmidt number,  $Sc$

## 6.6 Conclusions:

In this paper we have studied analytically the porosity and chemical reaction effects on an unsteady MHD free convection and mass transfer flow past a semi-infinite vertical plate embedded in a Darcian porous medium. From the present study the following conclusions can be drawn:

- An increase in magnetic field parameter decreases the velocity profiles.
- The velocity profiles are increased with an increase of free convection currents and porosity of the medium as well.
- The generative chemical reaction of the species leads to decrease of the flow velocity as well as concentration boundary layer.
- Large Darcy number (large porosity of the medium) leads to the increase of the velocity of the fluid within the boundary layer.
- The Prandtl number for the temperature field leads to decrease the thermal boundary layer.
- The concentration boundary layer has been reduced for the effect of Schmidt number.